A sandwich finite element for the analysis of piezoelectric adaptive shells of revolution

Valérie Gorge — Ayech Benjeddou[1] — Roger Ohayon

Conservatoire National des Arts et Métiers, Chaire de Mécanique,
2 rue Conté, F-75003 Paris

{gorge, benjedou, ohayon}@cnam.fr

ABSTRACT. *A simple finite element is proposed for the analysis of axisymmetric sandwich shells with piezoelectric faces. The latter are assumed through-thickness polarised and fully covered with electrodes on their inner and outer surfaces. Layerwise first-order shear deformation theory and displacement continuities at the sandwich interfaces are combined to reduce the mechanical unknowns to the faces mean and relative tangential displacements and bending rotations, augmented by the shell transverse deflection. Together with a layerwise linear electrical potential, these are first expanded with Fourier series along the shell circumference, then linearly interpolated along the meridian using Lagrange polynomials. Validation of the proposed piezoelectric sandwich conical finite element, through comparison with analytic free-vibration results available in the literature, has been found satisfactory.*

RÉSUMÉ. *Un élément fini simple est proposé pour l'analyse des coques axisymétriques sandwiches à peaux piézo-électriques. Ces dernières sont supposées polarisées suivant leurs épaisseurs et entièrement couvertes d'électrodes. La théorie de cisaillement de premier ordre discrète est combinée aux continuités des déplacements aux interfaces du sandwich pour réduire les inconnues mécaniques aux déplacements tangentiels et rotations de flexions moyens et relatifs des faces, augmentées de la flèche de la coque. Avec un potentiel électrique linéaire par couche, ces variables sont d'abord décomposées en séries de Fourier, puis interpolées linéairement suivant le méridien par les polynômes de Lagrange. La validation de l'élément fini conique, sandwich et piézo-électrique proposé, à travers la comparaison à des résultats en vibration libre disponibles dans la littérature, a été trouvée satisfaisante.*

KEYWORDS: *Sandwich structures, finite elements, piezoelectric materials, axisymmetric shells.*

MOTS-CLÉS : *structures sandwich, élément finis, matériaux piézo-électriques, coques axisymétriques*

[1]. Corresponding author.

REEF – 11/2002. Giens'01, pages 217 à 231

1. Introduction

A considerable amount of literature has been reported on the finite element (FE) modelling of smart structures (Mackerle, 1998, 2001 ; Benjeddou, 2000). However, despite of the relative maturity reached, only few piezoelectric FE have concerned axisymmetric shells, such as tubes (Ro *et al.*, 1997), cylinders (de Faria *et al.*, 1998), spherical caps (Wu *et al.*, 2001), and shells of revolution with arbitrary meridian (Correia *et al.*, 1999 ; Saravanan *et al.*, 2000, 2001).

The analysis of above mentioned FE literature indicates that, except that of Ro *et al.* (1997) for cylindrical shells only, all of them are based on the mixed equivalent single layer (ESL), for the mechanical behaviour, and layerwise approximation of the electrical potential. However, it is well known (Benjeddou *et al.*, 1996) that sandwich structures are characterised by the transverse shear deformation due to the relative motion of the faces against the core. Thus, a full layerwise (or discrete) modelling is necessary for adaptive shells with surface-bonded or embedded piezoelectric sensors and actuators. A simple FE has then been proposed recently by the present authors (Benjeddou *et al.*, 2001ab) for axisymmetric sandwich shells with a piezoelectric core, polarised along its meridian. Layerwise first-order shear deformation theory (FSDT) and linear electrical potential were considered for the FE formulation. The shell deflection and the faces mean and relative tangential displacements and bending rotations were retained as the independent mechanical variables. Interpolating all geometrical, mechanical and electrical variables with linear Lagrange polynomials has resulted in a cost-effective FE with nine mechanical and two electrical dof per node.

The present work, extends the previous one (Benjeddou *et al.*, 2001ab) to axisymmetric sandwich shells with through-thickness polarised piezoelectric faces. Using the same mechanical and FE formulations leads to a new simple FE with nine mechanical but four electrical dof per node. Hence the following theoretical and FE formulations will focus only on the piezoelectric and electrical contributions.

2. Theoretical formulation

The piezoelectric adaptive axisymmetric shell considered here is represented by its meridian section in Figure 1. It is composed of an elastic core sandwiched between two piezoelectric faces, representing surface-bonded actuators and sensors. Its theoretical formulation is based on the same *a priori* assumptions as in (Benjeddou *et al.*, 2001a), except the following ones :

– elastic core and piezoelectric faces are considered orthotropic with axes of material symmetry coinciding with the sandwich shell main curvatures,

– piezoelectric faces are through-thickness polarised, fully covered with electrodes on their inner and outer surfaces, but without electrodes on their edges,

– the electrical potential is assumed linear through each piezoelectric face thickness, but not necessary uniform.

Figure 1. *A meridian plane section of the piezoelectric sandwich axisymmetric shell*

2.1. *Kinematics*

As in (Benjeddou *et al.*, 1996 ; Benjeddou *et al.*, 2001a), the shell deflection and the faces mean and relative tangential displacements and bending rotations are retained as the independent mechanical variables. The latter have the general form :

$$\overline{x} = (x^a + x^b)/2 \quad ; \quad \tilde{x} = (x^a - x^b) \qquad [1]$$

where x= *u, v,* β, β_θ representing the tangential displacements in *s*, θ directions, and bending rotations in the planes *s*-*z* and θ-*z*, respectively. The shell tangential displacements are layerwise linear and continuous at the sandwich interfaces. When, they are written in terms of these variables (Benjeddou *et al.*, 2001a), then substituted in the usual FSDT strain-displacement relations, they lead to the following f^{th} face in-plane and transverse shear strains, respectively :

$$\{\varepsilon^f\} = (\{\overline{e}\} + \{\tilde{e}\}/2) + (z - z_f)(\{\overline{\kappa}\} + \{\tilde{\kappa}\}/2), \{\gamma^f\} = (\{\overline{\gamma}\} + \{\tilde{\gamma}\}/2) \qquad [2]$$

where $z_f = \pm(h_f + h_c)/2$; the '+' sign is for the inner face ($f = a$) and the '-' for the outer one ($f = b$). Mean and relative membrane ($\{\overline{e}\}, \{\tilde{e}\}$), bending ($\{\overline{\kappa}\}, \{\tilde{\kappa}\}$) and shear ($\{\overline{\gamma}\}$, $\{\tilde{\gamma}\}$) strain vectors are given in Appendix A. Similarly, the in-plane and transverse shear strains in the core can be written in the following form :

$$\{\varepsilon^c\} = (\{\overline{e}\} + \frac{\tilde{h}}{4}\{\overline{\kappa}\} + \frac{\overline{h}}{4}\{\tilde{\kappa}\}) + \frac{z}{h_c}(\{\tilde{e}\} + \overline{h}\{\overline{\kappa}\} + \frac{\tilde{h}}{4}\{\tilde{\kappa}\}), \{\gamma^c\} = (\{\overline{\gamma}^c\} + \{\tilde{\gamma}^c\}) \qquad [3]$$

where $\overline{h}$, $\tilde{h}$ are the mean and relative faces thickness parameters, defined as in [1]. The core mean and relative transverse shear strains (see Appendix A) are mainly due

to the relative displacements of the faces against the core, which can be explicitly represented only by the present independent variables. This motivates the decompositions into mean and relative quantities in the rest of the formulation.

2.2. *Electrical potentials and fields*

Following the last assumption, the electrical potential in the f^{th} piezoelectric face is :

$$\varphi^f(s,\theta,z) = \overline{\varphi}^f(s,\theta) + (z - z_f)\tilde{\varphi}^f(s,\theta)/h_f \qquad [4]$$

where $\overline{\varphi}^f$, $\tilde{\varphi}^f$ follow notations [1] for the prescribed or generated potentials φ^+ and φ^- on the inner and outer surfaces of the f^{th} face layer, respectively.

Substitution of equation [4] in the usual electrical field-potential relation gives the tangential and transverse electrical fields in the f^{th} piezoelectric face :

$$\{E_p^f\} = \{\overline{E}^f\} + (z - z_f)\{\tilde{E}^f\},\ E_z^f = -\tilde{\varphi}^f/h_f \qquad [5]$$

with

$$\{E_p^f\} = \{E_s^f \quad E_\theta^f\},\ \{\overline{E}^f\} = \{\overline{E}_s^f \quad \overline{E}_\theta^f\},\ \{\tilde{E}^f\} = \{\tilde{E}_s^f \quad \tilde{E}_\theta^f\}$$

$$\overline{E}_s^f = -\overline{\varphi}_{,s}^f,\ \overline{E}_\theta^f = -\frac{1}{r}\overline{\varphi}_{,\theta}^f,\ \tilde{E}_s^f = -\frac{1}{h_f}\tilde{\varphi}_{,s}^f,\ \tilde{E}_\theta^f = -\frac{1}{h_f r}\tilde{\varphi}_{,\theta}^f$$

Notice that, for uniform electrical potential, tangential electrical fields are nil.

2.3. *Reduced constitutive equations*

The reduced constitutive equations of through-thickness polarised piezoelectric materials result from considering zero transverse normal stress into the classical ones. Hence, the in-plane (p) and transverse (s) converse piezoelectric reduced constitutive equations in the f^{th} face are :

$$\{\sigma^f\} = [Q^f]\{\varepsilon^f\} - \{e_p^f\}E_z^f,\ \{\tau^f\} = [Q_s^f]\{\gamma^f\} - [e_s^f]^T\{E_p^f\} \qquad [6]$$

The plane and shear elastic matrices $[Q^f]$, $[Q_s^f]$ were given in (Benjeddou *et al.*, 2001a) and the piezoelectric ones $\{e_p^f\}$, $[e_s^f]$ are provided in Appendix B.

The plane and transverse direct piezoelectric reduced constitutive equations are given by the following electrical displacement relations :

$$\{D_p^f\} = [e_s^f]\{\gamma^f\} + [\eta_p^f]\{E_p^f\},\ D_z^f = e_p^f\{\varepsilon^f\} + \eta_{zz}^f E_z^f \qquad [7]$$

$[\eta_p^f]$, η_{zz}^f are modified dielectric plane matrix and transverse constant (Appendix B).

The reduced elastic constitutive equations of the core are deduced from [6] by substituting the superscript *f* by *c* and vanishing the piezoelectric matrices.

2.4. *Variational formulation*

For admissible virtual mean and relative displacements and rotations $\delta\bar{u}$, $\delta\bar{v}$, δw, $\delta\bar{\theta}$, $\delta\bar{\theta}_\eta$, $\delta\tilde{u}$, $\delta\tilde{v}$, $\delta\tilde{\theta}$, $\delta\tilde{\theta}_\eta$ and electrical potentials $\delta\bar{\varphi}^f$, $\delta\tilde{\varphi}^f$ ($f = a, b$), the extended d'Alembert principle (Benjeddou, 2000), applied to piezoelectric adaptive sandwich shells, can be written as :

$$\delta W_{int} - \delta W_{in} - \delta W_{ext} = 0 \qquad [8]$$

δW_{int}, δW_{in}, δW_{ext} are the sandwich shell internal, inertia and external virtual works. The last two terms were detailed in (Benjeddou *et al.*, 2001a) and are not repeated here for shortness. In the absence of applied body and surface electrical charges, the piezoelectric coupling is present only in the internal virtual work which can be written for the adaptive shell in hand as :

$$\begin{aligned}\delta W_{int} = &\sum_{k=a}^{c}\int_{\Omega^k}\left(\delta\bar{\varepsilon}^{k\,T}\bar{\sigma}^k + \delta\tilde{\varepsilon}^{k\,T}\tilde{\sigma}^k\right)d\Omega^k \\ &-\sum_{f=a}^{b}\int_{\Omega^f}\left(\delta E_p^{f\,T}D_p^f + \delta E_z^f D_z^f\right)d\Omega^f\end{aligned} \qquad [9]$$

where Ω^k is the domain volume of the kth layer. Taking into account the reduced piezoelectric constitutive equations [6,7] and decomposing the internal virtual work into mechanical (*m*), piezoelectric (*p*) and electrical (*e*) contributions, [9] becomes :

$$\delta W_{int} = \delta W_{int}^m + \delta W_{int}^p + \delta W_{int}^e \qquad [10]$$

with

$$\delta W_{int}^m = \sum_{k=a}^{c}\int_{\Omega^k}\left(\delta\bar{\varepsilon}^{k\,T}[Q^k]\bar{\varepsilon}^k + \delta\tilde{\varepsilon}^{k\,T}[Q_s^k]\tilde{\varepsilon}^k\right)d\Omega^k$$

$$\begin{aligned}\delta W_{int}^p = &\sum_{f=a}^{b}\Big(\int_{\Omega^f}\left(\delta\bar{\varepsilon}^{f\,T}d_p^f E_z^f + \delta\bar{\varepsilon}^{f\,T}[e_s^f]E_p^f\right)d\Omega^f \\ &+\int_{\Omega^f}\left(\delta E_z^f e_p^{f\,T}\bar{\varepsilon}^f + \delta E_p^{f\,T}[e_s^f]^T\tilde{\varepsilon}^f\right)d\Omega^f\Big)\end{aligned}$$

$$\delta W_{int}^e = \sum_{f=a}^{b}\int_{\Omega^f}\left(\delta E_p^{f\,T}[\varepsilon_p^f]E_p^f + \delta E_z^f\varepsilon_{zz}^f E_z^f\right)d\Omega^f$$

The mechanical contribution in [10] has been already (Benjeddou *et al.*, 2001a ; Benjeddou *et al.*, 1996) expressed in terms of the mean and relative strains [2,3].

2.4.1. *Piezoelectric virtual work*

Substituting equations [2,3,5], then integrating analytically through each piezoelectric face thickness, the piezoelectric virtual work, defined in [10], can be further decomposed into extension (e) and transverse shear (γ) contributions so that :

$$\delta W_{int}^{p} = \sum_{f=a}^{b} (\delta W_{e}^{pf} + \delta W_{\gamma}^{pf}) \qquad [11]$$

This expression shows that there is no electromechanical coupling due to the bending of the piezoelectric faces. Moreover, if the latter are so thin that they do not resist to transverse shear effects, as often assumed in the literature, the piezoelectric virtual work will reduce to its extension contribution only, leading to the conventional *extension actuation mechanism* (Benjeddou *et al.*, 2000).

The *extension contribution* of the piezoelectric virtual work comes from the coupling between the extension (membrane) strains and transverse electrical field :

$$\begin{aligned} \delta W_{e}^{pf} = & \int_{A^f} (\delta \bar{e} - \bar{D}_{e}^{pf} \delta \bar{\chi}_{z}^{f} - \bar{E}_{z}^{f} \delta \bar{D}_{e}^{pf} - \bar{\chi}_{z}^{f} \delta \bar{E}_{z}^{f}) dA^{f} \\ & + \int_{A^f} (\delta \tilde{e} - \tilde{D}_{e}^{pf} \delta \bar{\chi}_{z}^{f} - \bar{E}_{z}^{f} \delta \tilde{D}_{e}^{pf} - \tilde{\chi}_{z}^{f} \delta \bar{E}_{z}^{f}) dA^{f} \end{aligned} \qquad [12]$$

with $\bar{D}_{e}^{pf} = h_f e_{p}^{f}$, $\tilde{D}_{e}^{pf} = -\frac{1}{2} \bar{D}_{e}^{pf}$; ('+' for $f = a$, '-' for $f = b$)

Equation [12] indicates that extension-based electromechanical coupling is the sum of those between *transverse electrical field* and *mean and relative extension* strains. For an *actuation problem*, equation [12] reduces to :

$$\delta W_{e}^{pf} = \int_{A^f} (-\delta e^{f} + h_f \delta d_{p}^{f} \bar{\chi}_{z}^{f}) dA^{f} \qquad [13]$$

Writing the extension strains and transverse electrical field in terms of the face displacements and applied voltage $\tilde{V}^{f}$, respectively, transforms equation [13] to :

$$\delta W_{e}^{pf} = \int_{A^f} [(\frac{\partial \delta u^{f}}{\partial s} + \frac{\delta w}{R_s}) \hat{e}_{31}^{f} + (\frac{\cos\theta}{r} \delta u^{f} + \frac{1}{r} \frac{\partial \delta v^{f}}{\partial \theta} + \frac{\delta w}{R_\theta}) \hat{e}_{32}^{f}] \tilde{V}^{f} \, dA^{f} \qquad [14]$$

This equation shows that the shell curvatures introduce a membrane-bending coupling, which should be handled with great care, when the classical pin-force model is used, as is sometimes done (Lalande *et al.*, 1995) in the literature.

The *transverse shear contribution* of the piezoelectric virtual work comes from the coupling between the *mean and relative transverse shear strains* and the *mean plane electrical field* (due to the mean electrical potential) :

$$\delta W_{\phi}^{pf} = \int_{A^f} (\delta \bar{\gamma}^f - [\bar{D}_{\phi}^{pf}]^T \delta \bar{E}^f) + (\delta \tilde{\gamma}^f - [\tilde{D}_{\phi}^{pf}]^T \delta \bar{E}^f) \, dA^f \qquad [15]$$

with $[\bar{D}_{\phi}^{pf}] = h_f [e_s^f]^T$, $[\tilde{D}_{\phi}^{pf}] = \pm \frac{1}{2} [\bar{D}_{\phi}^{pf}]$; (‘+’ for $f = a$, ‘-‘ for $f = b$).

This virtual work vanishes for *uniform electrical potential* or *thin faces*, for which the transverse shear can be neglected. For the *actuation problem*, [15] reduces to :

$$\delta W_{\phi}^{pf} = \int_{A^f} (\delta \bar{\gamma}^f - h_f [e_s^f]^T \delta \bar{E}^f) \, dA^f \qquad [16]$$

Writing the transverse shear strains and plane electrical field in terms of the face displacements and applied voltage $\bar{\phi}^f$, respectively, transforms equation [16] to :

$$\delta W_{\phi}^{pf} = h_f \int_{A^f} [(\delta \gamma_{sz}^f - \frac{\partial \delta w}{\partial s} - \frac{\delta u^f}{R_s}) e_{15}^f \frac{\partial \delta \bar{\phi}^f}{\partial s} - (\delta \gamma_{\theta z}^f - \frac{1}{r}\frac{\partial \delta w}{\partial \theta} - \frac{\delta v^f}{R_{\theta}}) e_{24}^f \frac{1}{r}\frac{\partial \delta \bar{\phi}^f}{\partial \theta}] \, dA^f \qquad [17]$$

This transverse shear contribution, depends not only on the piezoelectric constants, applied voltage and shell curvatures as in [14], but on the face thickness also. Besides, equations [14, 17] indicate that these contributions do not coexist because the *extension* one is present for *opposite-phase* potentials, whereas the *shear* one operates with *in-phase* potentials.

2.4.2. *Electrical virtual work*

Considering the electrical fields [5], the electrical virtual work can be written as :

$$\delta W_{int}^{e} = \sum_{f=a}^{b} \delta W^{ef} \qquad [18]$$

with

$$\delta W^{ef} = \int_{A^f} (\delta \bar{E}^f - [\bar{\alpha}_p^f] \delta \bar{\phi}^f + \delta \tilde{E}^f - [\tilde{\alpha}_p^f] \delta \bar{\phi}^f) \, dA^f - \int_{A^f} \delta E_z^f \, \bar{\sigma}_{zz}^f \, E_z^f \, dA^f$$

$$[\bar{\alpha}_p^f] = h_f [\alpha_p^f], \quad [\tilde{\alpha}_p^f] = \frac{h_f^3}{12} [\alpha_p^f], \quad \bar{\sigma}_{zz}^f = h_f \sigma_{zz}^f$$

Only the last integral in equation [18] remains for uniform electrical potentials.

3. Finite element discretization

The piezoelectric sandwich axisymmetric shell is meshed into conical FE such as that represented in Figure 2. The element meridian is considered straight to attenuate

the membrane locking phenomenon usually present in curvilinear low-order FE. The mid-plane cylindrical co-ordinates of the sandwich shell are interpolated using linear Lagrange polynomials, whereas the mechanical and electrical independent variables are first expanded using Fourier series along the element circumference, then interpolated linearly as the geometry (Benjeddou *et al.*, 2001b). In the following, only the symmetric Fourier components are retained and focus is made on the linear interpolation along the meridian which looks like :

$$X(s) = N_1(s)X_1 + N_2(s)X_2 = (1 - \frac{s}{L})X_1 + \frac{s}{L}X_2 \qquad [19]$$

where s, L are the curvilinear abscissa and element length, respectively. X is either of the co-ordinates or independent mechanical and electrical variables. X_α (α=1, 2) are the corresponding nodal dof. Since all quantities are decomposed into mean and relative contributions, these are interpolated separately using reduced dof vectors.

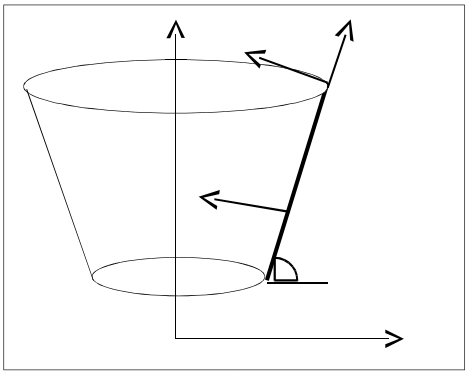

Figure 2. *The conical finite element*

The mechanical displacements discretization has been already presented in Benjeddou *et al.* (2001b). For shortness and as for the theoretical section, focus is made here on piezoelectric and electrical contributions only. However, for clarity, the discretization of membrane, bending and transverse shear strains is recalled :

$$\begin{aligned} \gamma &= [B3]d_t^e + z[B2]d_p^e + f[B2]d_r^e + f'[B2]d_r^e \\ \gamma &= [\bar{B}_s]d_t^e + f[\tilde{B}_s]d^e + [\bar{B}_s^c]d_t^e + f[\tilde{B}_s^c]d^e \end{aligned} \qquad [20]$$

with the strain derivative operator matrices given in (Benjeddou *et al.*, 2001b), and :

$$d_t^e = \{\bar{u}_1 \quad \bar{v}_1 \quad w_1 \quad \bar{u}_2 \quad \bar{v}_2 \quad w_2\}, \quad d_r^e = \{\bar{\theta}_1 \quad \bar{\theta}_{\varphi 1} \quad \bar{\theta}_2 \quad \bar{\theta}_{\varphi 2}\}$$

$$d^e = \{\bar{u}_1 \quad \bar{v}_1 \quad w_1 \quad \bar{\theta}_1 \quad \bar{\theta}_{\varphi 1} \quad \bar{u}_2 \quad \bar{v}_2 \quad w_2 \quad \bar{\theta}_2 \quad \bar{\theta}_{\varphi 2}\}$$

$$\tilde{d}_p^e = \{\tilde{u}_1 \quad \tilde{v}_1 \quad \tilde{u}_2 \quad \tilde{v}_2\}, \quad \tilde{d}_r^e = \{\tilde{\theta}_1 \quad \tilde{\theta}_{\varphi 1} \quad \tilde{\theta}_2 \quad \tilde{\theta}_{\varphi 2}\}$$

$$\tilde{d}^e = \{\tilde{u}_1 \quad \tilde{v}_1 \quad \tilde{\theta}_1 \quad \tilde{\theta}_{\varphi 1} \quad \tilde{u}_2 \quad \tilde{v}_2 \quad \tilde{\theta}_2 \quad \tilde{\theta}_{\varphi 2}\}$$

The symmetric Fourier series components of the mean and relative plane and transverse components of the electrical fields in the f^{th} piezoelectric face are interpolated along the shell meridian as :

$$\begin{Bmatrix} \tilde{E}_p^f \\ \tilde{E}_r^f \end{Bmatrix} = \begin{bmatrix} \bar{B}_p^f \end{bmatrix} \{\tilde{d}^{fe}\}, \quad \begin{Bmatrix} \tilde{E}_p^f \\ \tilde{E}_r^f \end{Bmatrix} = \begin{bmatrix} \tilde{B}_p^f \end{bmatrix} \{\tilde{d}^{fe}\}, \quad \tilde{E}_z^f = \hat{B}_p^f \{\tilde{d}^{fe}\} \qquad [21]$$

where

$$\{\tilde{d}^{fe}\} = \{\tilde{\varphi}_1^f \quad \tilde{\varphi}_2^f\}, \quad \{\tilde{d}^{fe}\} = \{\tilde{\varphi}_1^f \quad \tilde{\varphi}_2^f\}$$

The electrical field derivative operator matrices of the piezoelectric faces are similar to those given in (Benjeddou *et al.*, 2001b) for a piezoelectric core.

3.1. *Element stiffness matrix*

The element stiffness matrix results from the discretization of equation [9] :

$$\delta W_{int} = \delta d^e [k] \{d^e\} \qquad [22]$$

with

$$\{d^e\} = \{\bar{u}_1 \quad \bar{v}_1 \quad w_1 \quad \bar{\theta}_1 \quad \bar{\theta}_{\varphi 1} \quad \bar{\varphi}_1^a \quad \bar{\varphi}_1^b \quad \tilde{u}_1 \quad \tilde{v}_1 \quad \tilde{\theta}_1 \quad \tilde{\theta}_{\varphi 1} \quad \tilde{\varphi}_1^a \quad \tilde{\varphi}_1^b \quad \ldots$$
$$\ldots \quad \bar{u}_2 \quad \bar{v}_2 \quad w_2 \quad \bar{\theta}_2 \quad \bar{\theta}_{\varphi 2} \quad \bar{\varphi}_2^a \quad \bar{\varphi}_2^b \quad \tilde{u}_2 \quad \tilde{v}_2 \quad \tilde{\theta}_2 \quad \tilde{\theta}_{\varphi 2} \quad \tilde{\varphi}_2^a \quad \tilde{\varphi}_2^b\}$$

Following the decomposition of equation [10], the stiffness matrix is the sum of mechanical, piezoelectric and electrical contributions so that :

$$[k] = [k^m] + [k^p] + [k^e] \qquad [23]$$

where the last two matrices are derived from the separate discretization of the piezoelectric and electrical works, defined after equation [10]. The mechanical stiffness matrix has been detailed in (Benjeddou *et al.*, 2001b ; Benjeddou *et al.*, 1996).

3.1.1. *Piezoelectric stiffness matrix*

Following equation [11], the piezoelectric stiffness matrix is the sum of the extension and transverse shear contributions for each face. That is :

$$[k^p] = \sum_{f=a}^{b} [k^{pf}], \quad [k^{pf}] = [k_e^{pf}] + [k_\varphi^{pf}] \qquad [24]$$

Extension and transverse shear matrices are derived from the separate discretization of their virtual works. Hence, combining [12] and [20, 21], gives :

$$\begin{aligned} W_e^{pf} &= \bar{d}_t^e \, [\bar{k}_e^{pf}] \, \bar{d}^{fe} + \bar{d}^{fe} \, [\bar{k}_e^{pf}]^T \, \bar{d}_t^e \\ &+ \tilde{d}_p^e \, [\tilde{k}_e^{pf}] \, \bar{d}^{fe} + \bar{d}^{fe} \, [\tilde{k}_e^{pf}]^T \, \tilde{d}_p^e \end{aligned} \qquad [25]$$

These extension bloc-matrices are given in Appendix C. Their assembly, according to the element dof vector <d^e> [22], provides the face extension matrix. Similarly, the face transverse shear element matrix is the assembly of the transverse shear bloc-matrices, also given in Appendix C, resulting from the discretization of equation [15] using [20, 21] :

$$\begin{aligned} W_\gamma^{pf} &= \bar{d}^e \, [\bar{k}_\gamma^{pf}] \, \bar{d}^{fe} + \bar{d}^{fe} \, [\bar{k}_\gamma^{pf}]^T \, \bar{d}^e \\ &+ \tilde{d}^e \, [\tilde{k}_\gamma^{pf}] \, \bar{d}^{fe} + \bar{d}^{fe} \, [\tilde{k}_\gamma^{pf}]^T \, \tilde{d}^e \end{aligned} \qquad [26]$$

3.1.2. *Electrical stiffness matrix*

Following [18], the electrical stiffness matrix is the sum of the faces ones :

$$[k^e] = \sum_{f=a}^{b} [k^{ef}] \qquad [27]$$

where each face element matrix is the assembly, according to the element dof vector <d^e> [22], of the bloc-matrices (see Appendix C) resulting from the discretization of the electrical virtual work (defined after [18]) using equations [20] and [21] :

$$W^{ef} = \bar{d}^{fe} \, [\bar{k}^{ef}] \, \bar{d}^{fe} + \bar{d}^{fe} \, [\tilde{k}^{ef}] \, \bar{d}^{fe} + \bar{d}^{fe} \, [\hat{k}^{ef}] \, \bar{d}^{fe} \qquad [28]$$

For uniform electrical potentials, this equation reduces to its last term.

3.2. *Discrete equations of motion*

Mass matrices have been evaluated analytically (Benjeddou *et al.*, 2001b) while all stiffness matrices could be evaluated numerically using 3-point Gauss integration rule. However, to avoid shear locking phenomenon, 1-point Gauss rule was used for the transverse shear stiffness contributions. The previous theoretical and finite element formulations were derived in the shell local curvilinear basis. To take into account the shell meridian curvature and its eventual discontinuities, all stiffness and mass matrices and load vectors need to be transformed, prior to their assemblies, from the local to the global cylindrical co-ordinate system. After the assembly of the resulting global element stiffness, mass and load matrices, the discretization of the variational equation [8] takes the following standard form :

$$[M] \ddot{D} + [K] D = F \qquad [29]$$

where $\{D\}$ is the total dof vector of the piezoelectric sandwich shell. The aforementioned geometrical transformation introduces new relative deflection dof ; any resulting singularities in [29] could be avoided by enforcing the constant deflection assumption, introduced through penalisation of the relative radial and axial displacements at each node

$$\tilde{U}\sin\theta_0 - \tilde{W}\cos\theta_0 = 0 \qquad [30]$$

After splitting the dof vector of [29] into mechanical $\{q\}$ and electrical $\{\varphi\}$ dof sub-vectors, the following harmonic eigenvalue problem with circular frequency ω is derived for validation purpose :

$$\begin{bmatrix} K_{qq} & K_{q\varphi} \\ K_{q\varphi}^T & K_{\varphi\varphi} \end{bmatrix} - \omega^2 \begin{bmatrix} M & 0 \\ 0 & 0 \end{bmatrix} \begin{Bmatrix} q \\ \varphi \end{Bmatrix} = \begin{Bmatrix} 0 \\ 0 \end{Bmatrix} \qquad [31]$$

This large system is reduced by condensing the electrical nodal dof, $\{\varphi\} = -[K_{\varphi\varphi}]^{-1}[K_{q\varphi}]^T \{q\}$, so that only this standard eigenvalue problem is solved :

$$([K^*] - \omega^2[M])\{q\} = \{0\}, \quad [K^*] = [K_{qq} - K_{q\varphi} K_{\varphi\varphi}^{-1} K_{q\varphi}^T] \qquad [32]$$

4. Validation

The piezoelectric sandwich axisymmetric FE is now validated through vibration analysis of a clamped 0.6m-radius sandwich circular plate with 1mm-thick PZT-4 faces and 2cm-thick steel core. Material properties are those given by Wang *et al.* (2001) who have presented recently *analytic* modal characteristics of this plate. They considered a parabolic electrical potential in each piezoceramic face in the frame of Kirchhoff thin plate model. Here, 20 of the present FE were used to compute the lowest first 4 modes for open-circuited (OC) and short-circuited (SC) electrodes of the piezoceramic faces (Table 1). Obtained results indicate that OC electrical boundary conditions have more influence on the plate frequencies than SC ones. For the latter, the difference between analytic and FE values may be due to the electrical potential distribution assumption which is linear for the present FE, but parabolic for the analytic solution ; thus considering the induced potential due to the direct piezoelectric effect. This may explain the fact that the FE results of the OC electrical boundary conditions are closest to the analytic (SC) results than do the SC FE ones. FE results are within 1% and 5% for the OC and SC electrical boundary conditions, respectively. OC and SC frequency differences are less than 6%.

Mode (m, j)		(1,0)	(1,1)	(1,2)	(2,0)
Elastic	Analytic (Wang *et al.* , 2001)	138.42	288.05	472.59	538.85
	Present FE	138.21	287.34	470.76	538.93
	100 (FE-analytic)/analytic, %	-0.15	-0.25	-0.39	0.01

SC	Analytic (Wang *et al.* , 2001)	143.63	298.92	490.37	559.18
	Present FE	136.95	284.76	466.59	534.15
	100 (FE-analytic)/analytic, %	-4.65	-4.74	-4.85	-4.47
	Analy: 100 (piezo-elastic)/elastic, %	*3.77*	*3.76*	*3.77*	*3.77*
	FE: 100 (piezo-elastic)/elastic, %	*-0.91*	*-0.90*	*-0.89*	*-0.89*
OC	Present FE	145.04	301.41	493.60	564.94
	100 (FE-analytic)/analytic, %	0.98	0.83	0.66	1.03
	FE: 100 (piezo-elastic)/elastic, %	*4.94*	*4.90*	*4.85*	*4.83*
	FE: 100 (OC-SC)/SC, %	5.91	5.85	5.79	5.76

Table 1. *Lowest 4 frequencies (Hz) of a clamped sandwich circular plate with PZT-4 faces*

The influence of the piezoceramic face to elastic core thickness ratio (h_f/h_c) has been studied, for the SC but simply-supported (SS) above circular plate, by varying the face thickness while maintaining that of the core constant. Table 2 shows the lowest four frequencies obtained analytically by Wang *et al.* (2001) and using 20-FE of the present. It is found that the plate frequencies augment with the face to core thickness ratio. The FE results are within 5% of the analytical ones, except for the highest ratio, corresponding to the thicker face case, where the difference exceeds 6%. This may be due to the limitation of the Kirchhoff thin plate model used for the analytical solution. For the latter ratio, it is well known that the Reissner model, used in the FE solution, should behave better.

h_f/h_c	Mode (m, j)	(1,0)	(1,1)	(1,2)	(2,0)
1/12	Analytic (Wang *et al.* , 2001)	68.79	193.8	357.20	414.47
	Present FE	67.61	190.00	349.35	407.69
	100 (FE-analytic)/analytic, %	-1.71	-1.96	-2.20	-1.64
1/10	Analytic (Wang *et al.* , 2001)	69.33	195.36	360.08	417.82
	Present FE	67.82	190.56	350.35	417.81
	100 (FE-analytic)/analytic, %	-2.18	-2.46	-2.70	-2.14
1/8	Analytic (Wang *et al.* , 2001)	70.25	197.98	364.91	423.43
	Present FE	68.13	191.46	351.99	410.79
	100 (FE-analytic)/analytic, %	-3.01	-3.29	-3.54	-2.98
1/5	Analytic (Wang *et al.* , 2001)	73.58	207.42	382.34	443.65
	Present FE	69.30	194.69	357.81	417.69
	100 (FE-analytic)/analytic, %	-5.82	-6.14	-6.41	-5.85

Table 2. *Lowest 4 frequencies of a SS sandwich circular plate with variable thickness SC PZT-4 faces*

5. Conclusion

An adaptive sandwich axisymmetric shell element with piezoelectric faces has been formulated and validated. It has no derivative deflection dof thanks to the combination of layerwise FSDT assumptions and linear Lagrange interpolations of all mechanical and electrical independent variables. This nice feature is particularly suitable for interior noise reduction applications (structural-acoustic problems). By considering viscoelastic damping in the core, hybrid piezoelectric (active) – viscoelastic (passive) vibration control could be also studied with the present FE.

6. References

Benjeddou A., "Advances in piezoelectric finite element modelling of adaptive structural elements : a survey", *Computers and Structures*, vol. 76, no. 1-3, 2000, p. 347-363.

Benjeddou A., Gorge V., Ohayon R., "Use of piezoelectric shear response in adaptive sandwich shells of revolution – Part 1 : theoretical formulation", *Journal of Intelligent Material Systems and Structures*, vol. 12, no. 4, 2001a, p. 235-245.

Benjeddou A., Gorge V., Ohayon R., "Use of piezoelectric shear response in adaptive sandwich shells of revolution – Part 2 : finite element implementation", *Journal of Intelligent Material Systems and Structures*, vol. 12, no. 4, 2001b, p. 247-257.

Benjeddou A., Hamdi M. A., "A B-spline finite element for the dynamic analysis of sandwich shells of revolution", *Engineering Computations*, vol. 13, no. 2-4, 1996, p. 240-262.

Benjeddou A., Trindade M. A., Ohayon R., "Piezoelectric actuation mechanisms for intelligent sandwich structures", *Smart Materials and Structures*, vol. 9, no. 3, 2000, p. 328-335.

Correia I. F. P., Soares C. M. M., Soares C. A. M., Herskovits J., "Development of semi-analytical axisymmetric shell models with embedded sensors and actuators", *Composite Structures*, vol. 47, 1999, p. 531-541.

De Faria A. R., De Almeida S. F. M., "Axisymmetric actuation of composite cylindrical thin shells with piezoelectric rings", *Smart Materials and Structures*, vol. 7, 1998, p. 843-850.

Lalande F., Chaudhry Z., Rogers C. A., "Modelling considerations for in-phase actuation of actuators bonded to shell structures", *AIAA Journal*, vol. 33, 1995, p. 1300-1305.

Mackerle J., "Smart materials and structures – a finite element approach: a bibliography (1986-1997)", *Modelling and Simulation in Material Science and Engineering*, vol. 6, 1998, p. 293-334.

Mackerle J., "Smart materials and structures – FEM and BEM simulations: a bibliography (1997-1999)", *Finite Elements in Analysis and Design*, vol. 37, 2001, p. 71-83.

Ro J., El-Din K. S., Baz A., "Vibration control of tubes with internally moving loads using active constrained layer damping", *Proceeding of Active/Passive Vibration Control of*

Non Linear Dynamics of Structures, W. W. Clark *et al.* (eds), ASME DE-95/AMD-223, 1997, p. 1-11.

Saravanan C., Ganesan N., Ramamurti V., "Analysis of active damping in composite laminate cylindrical shells of revolution with skewed PVDF sensors/actuators", *Composite Structures*, vol. 48, 2000, p. 305-318.

Saravanan C., Ganesan N., Ramamurti V., "Semi-analytical finite element analysis of active constrained layer damping in cylindrical shells of revolution", *Computers and Structures*, vol. 79, 2001, p. 1131-1145.

Wang Q., Quek S. T., Sun C. T., Liu X., "Analysis of piezoelectric coupled circular plate", *Journal of Sound and Vibration*, vol. 245, no. 3, 2001, p. 527-544.

Wu Y.-C., Heyliger P., "Free vibration of layered piezoelectric spherical caps", *Smart Materials and Structures*, vol. 10, 2001, p. 229-239.

Appendix

A. *Mean and relative strains of the sandwich shell*

The mean extension $\{\bar{e}\} = \{\bar{e}_s \quad \bar{e}_\theta \quad \bar{e}_{s\theta}\}$, bending $\{\bar{\kappa}\} = \{\bar{\kappa}_s \quad \bar{\kappa}_\theta \quad \bar{\kappa}_{s\theta}\}$ and transverse shear $\{\bar{\gamma}\} = \{\bar{\gamma}_{sz} \quad \bar{\gamma}_{\theta z}\}$ strain vectors have the components :

$$\bar{e}_s = \frac{\partial \bar{u}}{\partial s} - \frac{w}{R_s}, \quad \bar{e}_\theta = \frac{C}{r}\bar{u} + \frac{1}{r}\frac{\partial \bar{v}}{\partial \theta} - \frac{S}{r}w, \quad \bar{e}_{s\theta} = \frac{1}{r}\frac{\partial \bar{u}}{\partial \theta} + \frac{\partial \bar{v}}{\partial s} - \frac{C}{r}\bar{v} \qquad [A1]$$

$$\bar{\kappa}_s = -\frac{\partial \bar{\beta}}{\partial s}, \quad \bar{\kappa}_\theta = -\frac{C}{r}\bar{\beta} - \frac{1}{r}\frac{\partial \bar{\alpha}}{\partial \theta}, \quad \bar{\kappa}_{s\theta} = -\frac{1}{r}\frac{\partial \bar{\beta}}{\partial \theta} - \frac{\partial \bar{\alpha}}{\partial s} + \frac{C}{r}\bar{\alpha} \qquad [A2]$$

$$\bar{\gamma}_{sz} = \frac{\bar{u}}{R_s} + \frac{\partial w}{\partial s} - \bar{\beta}, \quad \bar{\gamma}_{\theta z} = -\frac{S}{r}\bar{v} + \frac{1}{r}\frac{\partial w}{\partial \theta} - \bar{\alpha} \qquad [A3]$$

with $C = \cos\psi$, $S = \sin\psi$, ψ is the shell meridian angle (Figure 1).

The relative extension, bending and transverse shear strains in the faces can be obtained from previous respective expressions by substituting the mean displacements and rotations with corresponding relative ones, except $\tilde{w} = 0$. However, the mean and relative transverse shear strains in the core are :

$$\bar{\gamma}^c_{sz} = \frac{\bar{u}}{R_s} + \frac{\partial w}{\partial s} + \left(\frac{\bar{h}}{h_c} + \frac{\tilde{h}}{4R_s}\right)\bar{\beta}, \quad \bar{\gamma}^c_{\theta z} = \frac{\bar{v}}{R_\theta} + \frac{1}{r}\frac{\partial w}{\partial \theta} + \left(\frac{\bar{h}}{h_c} + \frac{\tilde{h}}{4R_\theta}\right)\bar{\alpha}$$

$$\tilde{\gamma}^c_{sz} = \frac{\tilde{u}}{h_c} + \frac{1}{4}\left(\frac{\tilde{h}}{h_c} + \frac{\bar{h}}{R_s}\right)\tilde{\beta}, \quad \tilde{\gamma}^c_{\theta z} = \frac{\tilde{v}}{h_c} + \frac{1}{4}\left(\frac{\tilde{h}}{h_c} + \frac{\bar{h}}{R_\theta}\right)\tilde{\alpha}; \quad \frac{1}{R_\theta} = \frac{S}{r} \qquad [A4]$$

B. *Reduced piezoelectric constitutive equations*

Zero transverse stress assumption reduces the linear piezoelectric constitutive equations to those defined in equations [6, 7] with the following stress, strain and electrical field and displacement vectors, and piezoelectric and dielectric matrices :

$$\{\sigma\} = \{\sigma_s \quad \sigma_\theta \quad \sigma_{s\theta}\}, \{\varepsilon\} = \{\varepsilon_s \quad \varepsilon_\theta \quad \varepsilon_{s\theta}\}, \{E_p\} = \{E_s \quad E_\theta\}$$

$$\{\tau\} = \{\tau_{sz} \quad \tau_{\theta z}\}, \{\gamma\} = \{\gamma_{sz} \quad \gamma_{\theta z}\}, \{D_p\} = \{D_s \quad D_\theta\} \qquad [B1]$$

$$[e_s] = \begin{bmatrix} 0 & e_{15} \\ e_{24} & 0 \end{bmatrix}, [\varepsilon_p] = \begin{bmatrix} \varepsilon_{11} & 0 \\ 0 & \varepsilon_{22} \end{bmatrix}, \{e_p\} = \{\hat{e}_{31} \quad \hat{e}_{32} \quad 0\} \qquad [B2]$$

$$\hat{e}_{31} = e_{31} - e_{33}\frac{C_{13}}{C_{33}}, \hat{e}_{32} = e_{32} - e_{33}\frac{C_{23}}{C_{33}}, \hat{\varepsilon}_{33} = \varepsilon_{33} + e_{33}\frac{e_{33}}{C_{33}} \qquad [B3]$$

where $C_{ij}, e_{il}, \varepsilon_{kl}$ ($i, j = 1, \ldots, 6$; $k, l = 1, 2, 3$) are the elastic, piezoelectric and dielectric material constants. Indices 1, 2, 3, 4, 5, 6 state for s, θ, z, θz, sz, $s\theta$.

C. *Piezoelectric and dielectric stiffness bloc-matrices*

The mean and relative extension and transverse shear contributions to the piezoelectric stiffness matrix of the f^{th} face are, respectively :

$$[\bar{k}_e^{pf}] = \int_0^L [B3]^T [\bar{D}_e^{pf}] [\hat{B}_\theta^f] \, rds \, , \, [\tilde{k}_e^{pf}] = \int_0^L [B2]^T [\tilde{D}_e^{pf}] [\hat{B}_\theta^f] \, rds \qquad [C1]$$

$$[\bar{k}_\theta^{pf}] = \int_0^L [\bar{B}_s]^T [\bar{D}_\theta^{pf}] [\bar{B}_\theta^f] rds \, , \, [\tilde{k}_\theta^{pf}] = \int_0^L [\tilde{B}_s]^T [\tilde{D}_\theta^{pf}] [\bar{B}_\theta^f] rds \qquad [C2]$$

The mean and relative bloc-matrices of the f^{th} face electrical stiffness matrix are :

$$[\bar{k}^{ef}] = \int_0^L [\bar{B}_\theta^f]^T [\bar{\varepsilon}_p^f] [\bar{B}_\theta^f] rds \, , \, [\tilde{k}^{ef}] = \int_0^L [\tilde{B}_\theta^f]^T [\bar{\varepsilon}_p^f] [\tilde{B}_\theta^f] rds$$

$$[\hat{k}^{ef}] = \int_0^L [\hat{B}_\theta^f]^T \bar{\varepsilon}_{zz}^f [\hat{B}_\theta^f] \, rds \qquad [C3]$$

In equations (C1-C3), $\alpha = 2$ for circumference index $j = 0$, and $\alpha = 1$ otherwise.